PEG-CCP/CaP hybrid nanoparticles were prepared by simple mixing of the component solutions [18]. The initial solution of the prepared nanoparticles contains several ions, such as Ca^{2+}, that may perturb the normal body homeostasis when applied systemically [32], thereby requiring purification of the solution for removal of the ions before systemic administration. However, the CaP nanoparticles are likely to dissociate in lower ionic strength solutions due to an equilibrium shift [8–10]. Thus, a suitable buffer solution is necessary for maintaining nanoparticle structure after purification. Our previous work suggested that PEGylated CaP nanoparticles were tolerable to an extracellular ionic solution ($CaCl_2$ 2 mM, Na_2HPO_4 1 mM, Tris 25 mM, NaCl 140 mM, pH 7.4) as they effectively delivered siRNA into cultured cells in that solution. The calcium concentration of the extracellular ionic solution is similar to that of body fluids, suggesting that minimal perturbation to blood homeostasis following intravenous administration is expected.

Hybrid nanoparticle solutions were purified by an ultrafiltration method, which allows rapid exchange of the buffer solutions. The ultrafiltration (MWCO: 10 kDa) was performed with replacement of the original solution for nanoparticle preparation ($CaCl_2$ 100 mM, Na_3PO_4 0.3 mM, NaCl 28 mM, Tris 6.6 mM, HEPES 12 mM) with EC buffer ($CaCl_2$ 2 mM, Na_2HPO_4 1 mM, Tris 25 mM, NaCl 140 mM, pH 7.4). The arsenazo III dye-based colorimetric assay revealed that the ultrafiltration process removed 84% of the original calcium content, with residual calcium corresponding mostly to the calcium contained in nanoparticles. The resulting nanoparticles were characterized by DLS and AFM. Purified nanoparticles maintained a narrowly dispersed size distribution in the DLS (Z-weighted) histogram, similar to non-purified controls (Fig. 2A). Spherical morphologies with the similar size were observed in the AFM images of both purified and non-purified hybrid nanoparticles (Figs. 2B and C). These results indicate that purification for removal of excess calcium ions was successful, without alteration of hybrid nanoparticle structure.

Hybrid nanoparticle stability upon storage is also important for their quality control towards pharmaceutical applications. Thus, the size of hybrid nanoparticle was monitored over time by DLS following storage at 4 °C (Fig. 3). Non-purified hybrid nanoparticles did not show a significant change in both size and PdI for at least 168 h (7 days). Purified nanoparticle size remained similar to that of the non-purified control for the first 96 h and then the size slightly increased thereafter, possibly due to secondary aggregate formation. This aggregation can be explained by compromised colloidal stability of nanoparticles, triggered by PEG-CCP detachment from the nanoparticles associated with their gradual dissolution. These results suggest that the dissolution of the purified nanoparticle is intrinsically slow in the EC buffer.

3.2. Stability of hybrid nanoparticles in a serum-containing culture medium and a cytoplasmic ionic solution

Purified hybrid nanoparticle stability was further assessed in medium containing serum proteins. Nanoparticles were prepared with Cy5-labeled siRNA (Cy5-siRNA) and then subjected to fluorescence correlation spectroscopy (FCS) analysis. FCS analysis allows determination of the diffusion coefficient of siRNA-incorporating nanoparticles in the complex protein-containing solution without interference from non-labeled macromolecules or aggregates [33–35]. Note that the diffusion coefficient is inversely proportional to the hydrodynamic size of the fluorescent molecule based on the Stokes–Einstein equation for spherical particles; thus the size of nanoparticles can be determined. In conventional condition used for siRNA transfection (100 nM siRNA in 10% FBS medium), the initial size of nanoparticles was determined to be approximately 100 nm (Fig. 4A), which is consistent with the size in DLS histogram and AFM image of nanoparticles not exposed to biological media (Fig. 2). Additionally, size was maintained following 4 h incubation at 37 °C, indicating high tolerability in medium containing serum proteins.

In addition to high tolerability within extracellular conditions, delivery vehicles must finally release the encapsulated siRNA in the cytoplasm to gain access to the RNAi pathway. Hence, siRNA release from the hybrid nanoparticles was further evaluated by FCS in a solution mimicking the ionic condition of the cytoplasm ($CaCl_2$ 100 nM, Na_2HPO_4 40 mM, NaCl 140 mM, pH 7.4), as the dissolution of CaP nanoparticles should be significantly influenced by the concentration of calcium and phosphate ions. The average calcium ion concentrations are 2 mM and 100 nM in the blood and the cytoplasm, respectively. The lower calcium concentration in the cell cytoplasm may trigger selective intracellular release of siRNA from the CaP nanoparticles. Indeed, when nanoparticles were incubated in the cytoplasmic ionic solution, the size of the nanoparticles was drastically reduced within 1 h incubation, ultimately reaching the same value of naked siRNA (Fig. 4B), which is consistent with our previous findings regarding the dissolution behavior of hybrid nanoparticles [8].

3.3. In vitro gene silencing

The gene silencing activity of nanoparticles containing siVEGF was evaluated in cultured human pancreatic adenocarcinoma (BxPC3) cells. BxPC3 was chosen as a target cancer cell because of the fact that subcutaneous BxPC3 tumors exhibit poorly differentiated histology with thick fibrotic stromal tissue surrounding tumor nests [36], thereby resembling intractable tumors in clinical settings. As shown in Fig. 5, both non-purified and purified hybrid nanoparticles encapsulating siVEGF significantly reduced VEGF mRNA in comparison with controls incorporating siSCR. The reduction in VEGF mRNA was 71% and 63% for purified and non-purified nanoparticles, respectively. Strong gene silencing activity of hybrid nanoparticles is probably due to their high complex stability in the transfection medium (Fig. 4A) and selective siRNA release in the cell cytoplasm (Fig. 4B) as well as facilitated endosomal escape of siRNA by PEG-CCP, as extensively examined in previous studies [18,19]. No statistical difference was found between nanoparticle formulations, indicating that there was apparently no loss of the biological activity of siRNA after purification. Analysis of cell viability (CCK-8, Dojindo, Japan) showed no difference between nanoparticle-treated samples and controls at tested siRNA

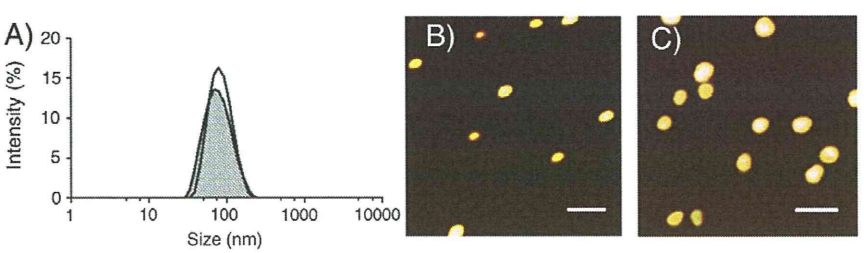

Fig. 2. (A) Size distribution of CaP nanoparticles before (filled curve) and after (open curve) purification by ultrafiltration, determined by DLS. (B, C) Atomic force microscopic images of non-purified (B) and purified (C) hybrid nanoparticles. Scale bar corresponds to 200 nm.

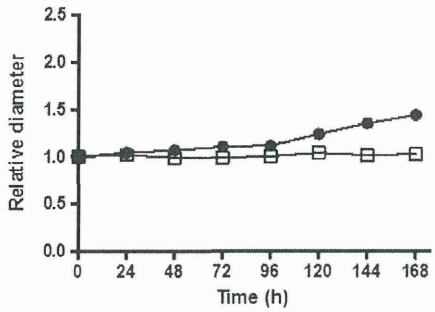

Fig. 3. Time-dependent change in the relative diameter of non-purified (open square) and purified (closed circle) hybrid nanoparticles, determined by DLS (temperature: 4 °C, siRNA concentration: 3 μM).

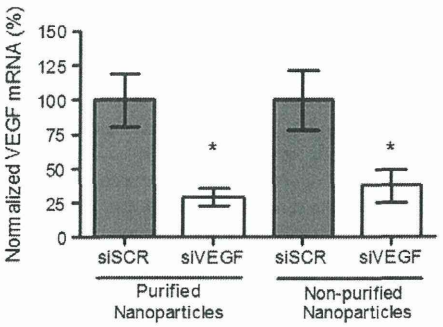

Fig. 5. Gene silencing activity of hybrid nanoparticles in cultured BxPC3 cells (siRNA concentration: 100 nM, incubation time: 24 h, $n=3$). *$p<0.05$ for the control incorporating siSCR (ANOVA followed by Newman–Keuls).

concentration (Supporting Fig. 2), indicating that VEGF silencing is due to the RNAi effect and not an artifact of toxicity.

3.4. Antitumor activity

Antitumor activity of siVEGF-incorporating hybrid nanoparticles was evaluated against a subcutaneous BxPC3 tumor model. Silencing of VEGF gene in tumor tissues can prevent angiogenesis, subsequently blocking the nutrient supply needed for tumor growth (antiangiogenic therapy). As presented in Fig. 6, tumors treated by I.V. injection of nanoparticles containing siVEGF showed suppressed growth, compared to those treated with nanoparticles containing siSCR as well as nanoparticles without siRNA and EC buffer only. A statistical significance was observed at days 3, 5, 7 and 9 for tumors treated with the siVEGF nanoparticles compared to controls. It is noteworthy that the significant tumor growth inhibition was observed after the first injection of the siVEGF nanoparticle. At day 9, the tumor volume in mice treated with the siVEGF nanoparticles was around 66% of the average volume of controls. I.V. injection of nanoparticles did not result in acute or severe toxicity, as no significant difference in body weight was observed between treated and control groups during the experimental period (data not shown). Additionally, blood levels of alanine aminotransferase (ALT) and aspartate aminotransferase (AST) were not significantly altered after I.V. injection of hybrid nanoparticles (Supporting Fig. 3), suggesting negligible acute toxicity associated with nanoparticle administration. These results demonstrate that the PEG-CCP/CaP hybrid nanoparticle with siVEGF is a promising formulation for cancer therapy.

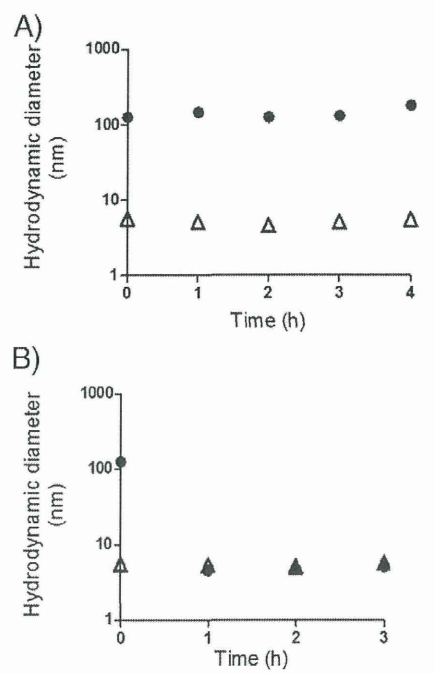

Fig. 4. Time-dependent change in hydrodynamic diameters of hybrid nanoparticles incorporating Cy5-siRNA (closed circle) and naked Cy5-siRNA (open triangle) determined by FCS in the medium containing 10% FBS (A) and in the medium mimicking the cytoplasm (Ca^{2+} and PO_4^{3-} concentrations were 100 nM and 40 mM, respectively) (B).

3.5. Accumulation of siRNA and gene silencing in tumors

In order to obtain further evidence that the antitumor activity of siRNA-containing hybrid nanoparticles was induced by the RNAi effect, accumulation of siRNA within subcutaneous tumors was evaluated. Hybrid nanoparticles were prepared with Cy5-siRNA and injected into mice in the similar manner used for tumor growth inhibition experiments. Mice were sacrificed and the tumors were excised 60 min after systemic administration of the hybrid nanoparticles, and Cy5 fluorescence was measured by IVIS. Fluorescence intensity was normalized to the tumor weight for quantitative evaluation. Significantly stronger fluorescence was detected in tumors treated with hybrid nanoparticles, compared to naked siRNA (Fig. 7A), indicating enhanced tumor accumulation of siRNA by hybrid nanoparticle delivery. Considering the fact that naked siRNA is immediately degraded in the bloodstream and subsequently cleared from kidney, the improved tumor accumulation may be due to suppressed siRNA degradation in the bloodstream as well as slower renal clearance of siRNA.

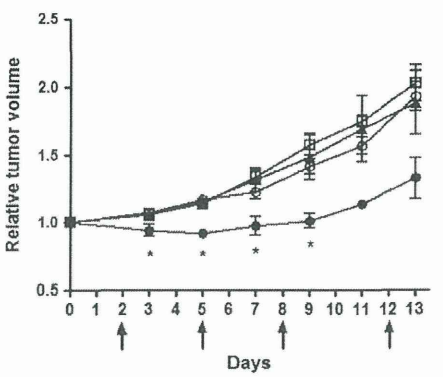

Fig. 6. Relative tumor volume of subcutaneous BxPC3 tumors treated by the hybrid nanoparticles with siVEGF (closed circle), with siSCR (closed triangle), hybrid nanoparticles without siRNA (open square) and EC buffer control (open circle) ($n=4$). Arrows indicate injection day (25 μg siRNA/injection). *$p<0.05$ for EC buffer control (ANOVA followed by Newman–Keuls).

Target gene mRNA levels were also evaluated as direct evidence for RNAi-based antitumor activity. In order to confirm VEGF mRNA degradation in tumor tissue, an additional injection of nanoparticles was performed to a separated group of mice bearing subcutaneous BxPC3 tumors ($n=3$). Approximately 1 day after the injection, mice were sacrificed and tumors were excised, followed by the extraction of RNA and real-time RT-PCR analysis. Fig. 7B clearly shows that significantly higher gene silencing activity (~68%) was achieved with hybrid nanoparticles containing siVEGF, compared to those prepared with siSCR as well as a buffer control. This result corroborates with the significant antitumor activity achieved with nanoparticles containing siVEGF (Fig. 6). Altogether, effective tumor accumulation and VEGF mRNA degradation strongly suggest that tumor growth suppression was a result of RNAi.

4. Conclusion

In this work, the *in vivo* application of PEG-CCP/CaP hybrid nanoparticles carrying siRNA was investigated for siRNA-based cancer treatment. Hybrid nanoparticles were submitted to purification for significant reduction of the amount of free calcium in solution. Purified hybrid nanoparticles were found to have the following characteristics: i) a similar size distribution and morphology to non-purified controls, ii) excellent tolerability in the serum-containing medium, iii) reversible capture of siRNA, with release in cytoplasmic ionic conditions. Efficient gene silencing activity without associated toxicity was also confirmed for nanoparticles in cultured BxPC3 cells. Intravenously injected nanoparticles incorporating VEGF siRNA led to significant reduction in tumor growth. Enhanced siRNA accumulation in subcutaneous BxPC3 tumors was found and subsequently induction of effective VEGF gene silencing in the tumor was observed. Based on the presented results, the PEG-CCP/CaP hybrid nanoparticles demonstrate great potential for clinical applications toward siRNA-based cancer therapies.

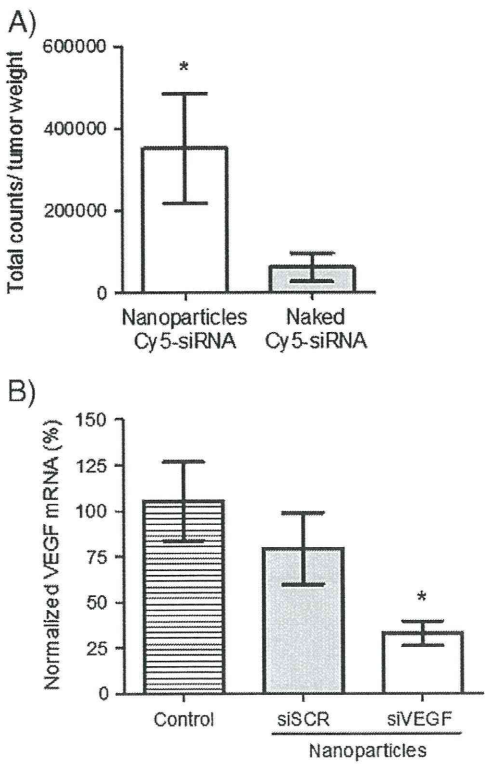

Fig. 7. (A) Accumulation of Cy5-siRNA in subcutaneous BxPC3 tumors 60 min after systemic administration. The Cy5 fluorescence intensity in the excised tumor tissue was determined by IVIS, followed by the normalization by the tumor weight ($n=5$). *$p<0.05$ for naked Cy5-siRNA (Mann–Whitney t test). (B) *In vivo* VEGF gene silencing activity in subcutaneous BxPC3 tumors 1 day after systemic administration of samples (25 μg siRNA), revealed by real-time RT-PCR ($n=3$). *$p<0.05$ for ionic buffer control (ANOVA followed by Newman–Keuls).

Acknowledgment

This research was granted by the Japan Society for the Promotion of Science (JSPS) through the "Funding Program for World-Leading Innovative R&D on Science and Technology (FIRST Program)," initiated by the Council for Science and Technology Policy (CSTP). The authors express their appreciation to Dr. M. Oba (Nagasaki University) and Dr. H. Cabral (The University of Tokyo) for the help in animal experiments.

Appendix A. Supplementary data

Supplementary data to this article can be found online at http://dx.doi.org/10.1016/j.jconrel.2012.05.005.

References

[1] A. Fire, S. Xu, M.K. Montgomery, S.A. Kostas, S.E. Driver, C.C. Mello, Potent and specific genetic interference by double-stranded RNA in *Caenorhabditis elegans*, Nature 391 (1998) 806–811.
[2] S.M. Elbashir, J. Harborth, W. Lendeckel, A. Yalcin, K. Weber, T. Tushl, Duplexes of 21-nucleotide RNAs mediate interference in cultured mammalian cells, Nature 411 (2001) 494–498.
[3] B.L. Davidson, P.B. McCray, Current prospects for RNA interference-based therapies, Nat. Rev. Genet. 12 (2011) 329–340.
[4] M.E. Davis, J.E. Zuckerman, C.H.J. Choi, D. Seligson, A. Tolcher, C.A. Alabi, Y. Yen, J.D. Heidel, A. Ribas, Evidence of RNAi in humans from systemically administered siRNA via targeted nanoparticles, Nature 464 (2010) 1067–1070.
[5] A. Maitra, Calcium phosphate nanoparticles: second-generation nonviral vectors in gene therapy, Expert. Rev. Mol. Diagn. 5 (2005) 893–905.
[6] M. Zhang, K. Kataoka, Nano-structured composites based on calcium phosphate for cellular delivery of therapeutic and diagnostic agents, Nano Today 4 (2009) 508–517.
[7] Y. Kakizawa, K. Kataoka, Block copolymer self-assembly into monodispersive nanoparticles with hybrid core of antisense DNA and calcium phosphate, Langmuir 18 (2002) 4539–4543.
[8] Y. Kakizawa, S. Furukawa, K. Kataoka, Block copolymer-coated calcium phosphate nanoparticles sensing intracellular environment for oligodeoxynucleotide and siRNA delivery, J. Control. Release 97 (2004) 345–356.
[9] Y. Kakizawa, S. Furukawa, A. Ishii, K. Kataoka, Organic–inorganic hybrid-nanocarrier of siRNA constructing through the self-assembly of calcium phosphate and PEG-based block aniomer, J. Control. Release 111 (2006) 368–370.
[10] M. Zhang, A. Ishii, N. Nishiyama, S. Matsumoto, T. Ishii, Y. Yamasaki, K. Kataoka, PEGylated calcium phosphate nanocomposites as smart environment-sensitive carriers for siRNA delivery, Adv. Mater. 21 (2009) 3520–3525.
[11] E.V. Giger, J. Puigmartí-Luis, R. Schlatter, B. Castagner, P.S. Dittrich, J.C. Leroux, Gene delivery with bisphosphonate-stabilized calcium phosphate nanoparticles, J. Control. Release 150 (2011) 87–93.
[12] J. Li, Y.C. Chen, Y.C. Tseng, C. Mozumdar, L. Huang, Biodegradable calcium phosphate nanoparticle with lipid coating for systemic siRNA delivery, J. Control. Release 142 (2010) 416–421.
[13] V.V. Sokolova, I. Radtke, R. Heumann, M. Epple, Effective transfection of cells with multi-shell calcium phosphate DNA nanoparticles, Biomaterials 27 (2006) 3147–3153.
[14] Y. Matsumura, H. Maeda, A new concept for macromolecular therapeutics in cancer-chemotherapy: mechanisms of tumoritropic accumulation of proteins and the antitumor agent SMANCS, Cancer Res. 46 (1986) 6387–6392.
[15] S.M. Moghimi, A.C. Hunter, J.C. Murray, Long-circulating and target-specific nanoparticles: theory to practice, Pharm. Rev. 53 (2001) 283–318.
[16] K. Kataoka, A. Harada, Y. Nagasaki, Block copolymer micelles for drug delivery: design, characterization and biological significance, Adv. Drug Deliv. Rev. 47 (2001) 113–131.
[17] K. Miyata, R.J. Christie, K. Kataoka, Polymeric micelles for nano-scale drug delivery, React. Funct. Polym. 71 (2011) 227–234.
[18] F. Pittella, M. Zhang, Y. Lee, H.J. Kim, T. Tockary, K. Osada, T. Ishii, K. Miyata, N. Nishiyama, K. Kataoka, Enhanced endosomal escape of siRNA-incorporating hybrid nanoparticles from calcium phosphate and PEG-block charge-conversional polymer for efficient gene knockdown with negligible cytotoxicity, Biomaterials 32 (2011) 3106–3114.
[19] Y. Lee, K. Miyata, M. Oba, T. Ishii, S. Fukushima, M. Han, H. Koyama, N. Nishiyama, K. Kataoka, Charge-conversional ternary polyplex with endosome disruption moiety: a technique for efficient and safe gene delivery, Angew. Chem. Int. Ed. 47 (2008) 5163–5166.
[20] N. Kanayama, S. Fukushima, N. Nishiyama, K. Itaka, W.D. Jang, K. Miyata, Y. Yamasaki, U.I. Chung, K. Kataoka, A PEG-based biocompatible block catiomer with high buffering capacity for the construction of polyplex micelles

showing efficient gene transfer toward primary cells, ChemMedChem 1 (2006) 439–444.
[21] K. Miyata, M. Oba, M. Nakanishi, S. Fukushima, Y. Yamasaki, H. Koyama, N. Nishiyama, K. Kataoka, Polyplexes from poly(aspartamide) bearing 1,2-diaminoethane side chains induce pH-selective, endosomal membrane destabilization with amplified transfection and negligible cytotoxicity, J. Am. Chem. Soc. 130 (2008) 16287–16294.
[22] S. Takae, K. Miyata, M. Oba, T. Ishii, N. Nishiyama, K. Itaka, Y. Yamasaki, H. Koyama, K. Kataoka, PEG-detachable polyplex micelles based on disulfide-linked block catiomers as bioresponsive nonviral gene vectors, J. Am. Chem. Soc. 130 (2008) 6001–6009.
[23] K. Itaka, T. Ishii, Y. Hasegawa, K. Kataoka, Biodegradable polyamino acid-based polycations as safe and effective gene carrier minimizing cumulative toxicity, Biomaterials 31 (2010) 3707–3714.
[24] H. Uchida, K. Miyata, M. Oba, T. Ishii, T. Suma, K. Itaka, N. Nishiyama, K. Kataoka, Odd-even effect of repeating aminoethylene units in the side chain of N-substituted polyaspartamides on gene transfection profiles, J. Am. Chem. Soc. 133 (2011) 15524–15532.
[25] K. Miyata, N. Nishiyama, K. Kataoka, Rational design of smart supramolecular assemblies for gene delivery: chemical challenge in the creation of artificial viruses, Chem. Soc. Rev. 41 (2012) 2562–2574.
[26] N. Ferrara, VEGF as a therapeutic target in cancer, Oncology 69 (2005) 11–16.
[27] Y. Takei, K. Kadomatsu, Y. Yuzawa, S. Matsuno, T. Muramatsu, A small interfering RNA targeting vascular endothelial growth factor as cancer therapeutics, Cancer Res. 64 (2004) 3365–3370.
[28] E. Song, P. Zhu, S.K. Lee, D. Chowdhury, S. Kussman, D.M. Dykxhoorn, Y. Feng, D. Palliser, D.B. Weiner, P. Shankar, W.A. Marasco, J. Lieberman, Antibody mediated in vivo delivery of small interfering RNAs via cell-surface receptors, Nat. Biotechnol. 23 (2005) 709–717.
[29] W.J. Kim, L.V. Christensen, S. Jo, J.W. Yockman, J.H. Jeong, Y.H. Kim, S.W. Kim, Cholesteryl oligoarginine delivering vascular endothelial growth factor siRNA effectively inhibits tumor growth in colon adenocarcinoma, Mol. Ther. 14 (2006) 343–350.
[30] H.J. Kim, M. Oba, F. Pittella, T. Nomoto, H. Cabral, Y. Matsumoto, K. Miyata, N. Nishiyama, K. Kataoka, PEG-detachable cationic polyaspartamide derivatives bearing stearoyl moieties for systemic siRNA delivery toward subcutaneous BxPC3 pancreatic tumor, J. Drug Target. 20 (2012) 33–42.
[31] D.M. Euhus, C. Hudd, M.C. LaRegina, F.E. Johnson, Tumor measurement in the nude mouse, J. Surg. Oncol. 31 (1986) 229–234.
[32] A.W. Winkler, H.E. Hoff, P.K. Smith, Cardiovascular effects of potassium, calcium, magnesium, and barium: an experimental study of toxicity and rationale of use in therapeutics, Yale J. Biol. Med. 13 (1940) 123–132.
[33] K. Buyens, M. Meyer, E. Wagner, J. Demeester, S.C.D. Smedt, N.N. Sanders, Monitoring the disassembly of siRNA polyplexes in serum is crucial for predicting their biological efficacy, J. Control. Release 141 (2010) 38–41.
[34] H.J. Kim, A. Ishii, K. Miyata, Y. Lee, S. Wu, M. Oba, N. Nishiyama, K. Kataoka, Introduction of stearoyl moieties into a biocompatible cationic polyaspartamide derivative, PAsp(DET), with endosomal escaping function for enhanced siRNA-mediated gene knockdown, J. Control. Release 145 (2010) 141–148.
[35] H. Takemoto, A. Ishii, K. Miyata, M. Nakanishi, M. Oba, T. Ishii, Y. Yamasaki, N. Nishiyama, K. Kataoka, Polyion complex stability and gene silencing efficiency with a siRNA-grafted polymer delivery system, Biomaterials 31 (2010) 8097–8105.
[36] M.R. Kano, Y. Bae, C. Iwata, Y. Morishita, M. Yashiro, M. Oka, T. Fujii, A. Komuro, K. Kiyono, M. Kaminishi, K. Hirakawa, Y. Ouchi, N. Nishiyama, K. Kataoka, K. Miyazono, Improvement of cancer-targeting therapy, using nanocarriers for intractable solid tumors by inhibition of TGF-β signaling, Proc. Natl. Acad. Sci. U. S. A. 104 (2007) 3460–3465.

Targeted Polymeric Micelles for siRNA Treatment of Experimental Cancer by Intravenous Injection

R. James Christie,[†] Yu Matsumoto,[†,‡,§] Kanjiro Miyata,[†] Takahiro Nomoto,[⊥] Shigeto Fukushima,[∥] Kensuke Osada,[∥] Julien Halnaut,[¶] Frederico Pittella,[∥] Hyun Jin Kim,[∥] Nobuhiro Nishiyama,[†] and Kazunori Kataoka[†,⊥,∥,#,*]

[†]Division of Clinical Biotechnology, Center for Disease Biology and Integrative Medicine, Graduate School of Medicine and [‡]Department of Otorhinolaryngology and Head and Neck Surgery, Graduate School of Medicine and Faculty of Medicine, The University of Tokyo, Japan, [§]Department of Otorhinolaryngology and Head and Neck Surgery, Mitsui Memorial Hospital, Japan, and [⊥]Department of Bioengineering and [∥]Department of Materials Engineering, Graduate School of Engineering, [¶]Center for Medical System Innovation, International Student Exchange Program, and [#]Center for NanoBio Integration, The University of Tokyo, Japan

ABSTRACT Small interfering ribonucleic acid (siRNA) cancer therapies administered by intravenous injection require a delivery system for transport from the bloodstream into the cytoplasm of diseased cells to perform the function of gene silencing. Here we describe nanosized polymeric micelles that deliver siRNA to solid tumors and elicit a therapeutic effect. Stable multifunctional micelle structures on the order of 45 nm in size formed by spontaneous self-assembly of block copolymers with siRNA. Block copolymers used for micelle formation were designed and synthesized to contain three main features: a siRNA binding segment containing thiols, a hydrophilic nonbinding segment, and a cell-surface binding peptide. Specifically, poly(ethylene glycol)-*block*-poly(L-lysine) (PEG-*b*-PLL) comprising lysine amines modified with 2-iminothiolane (2IT) and the cyclo-Arg-Gly-Asp (cRGD) peptide on the PEG terminus was used. Modification of PEG-*b*-PLL with 2IT led to improved control of micelle formation and also increased stability in the blood compartment, while installation of the cRGD peptide improved biological activity. Incorporation of siRNA into stable micelle structures containing the cRGD peptide resulted in increased gene silencing ability, improved cell uptake, and broader subcellular distribution *in vitro* and also improved accumulation in both the tumor mass and tumor-associated blood vessels following intravenous injection into mice. Furthermore, stable and targeted micelles inhibited the growth of subcutaneous HeLa tumor models and demonstrated gene silencing in the tumor mass following treatment with antiangiogenic siRNAs. This new micellar nanomedicine could potentially expand the utility of siRNA-based therapies for cancer treatments that require intravenous injection.

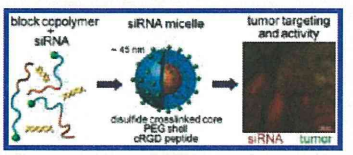

KEYWORDS: siRNA delivery · block copolymer · micelle · cRGD · cancer therapy

Small interfering ribonucleic acid (siRNA) therapeutics have great potential for treatment of disease through inhibition of protein expression, but transfer of this technology to the clinic has proven to be a great challenge. siRNA-based therapies block the expression of aberrant proteins using a natural subcellular pathway that degrades messenger RNA (mRNA) based on the nucleotide sequence contained in the siRNA molecule, a process known as RNA interference (RNAi).[1] siRNA is a 20–23 base pair degradation product generated from longer double-stranded RNA and represents the smallest double-stranded RNA deliverable that can gain access to the RNAi pathway. Potent inhibition of gene expression can be achieved due to the catalytic nature of RNAi, which results in formation of an activated RNA-induced silencing complex (RISC) that can degrade multiple strands of mRNA that are complementary to the loaded siRNA strand.[2]

The molecular machinery necessary for RNAi is located in the cell cytoplasm, thus therapeutic siRNA must also localize in the cytoplasm to exert the desired effect of protein knockdown. However, siRNA is a large water-soluble polyion (~13 000 MW) that has unique delivery obstacles not typically encountered with small hydrophobic molecules such as anticancer drugs. Due to its large size and anionic nature, siRNA cannot readily diffuse across cell membranes and requires active internalization into cells by endocytosis. Furthermore, administration of siRNA by systemic injection is challenging due to the immunogenicity of naked siRNA, degradation into inactive fragments by enzymatic activity, high renal clearance, and overall poor accumulation at target sites.[3–6] Efforts to overcome the above-mentioned obstacles has resulted in development of next-generation siRNA delivery strategies including chemically modified siRNAs that increase stability and suppress immune system activation, as well

* Address correspondence to kataoka@bmw.t.u-tokyo.ac.jp.

Received for review March 2, 2012 and accepted May 10, 2012.

Published online May 10, 2012
10.1021/nn300942b

as development of many types of particle-based systems that reversibly encapsulate siRNA. Particle-based systems are often designed to exploit the large polyanionic structure of siRNA to form polyion complexes which assemble into aggregates, vesicles, or micelles. Such particles have been prepared from cationic lipids, lipidoids, peptides, as well as synthetic polymers and block copolymers and are typically several tens to hundreds of nanometers in size. The most sophisticated delivery systems to date include features such as a PEG coating to control particle morphology and reduce nonspecific interactions with biological components, reversible cross-links for site-specific release of siRNA, environment-sensitive polymers or peptides to assist subcellular trafficking, and cell-targeting moieties to improve cell uptake and specificity. Several excellent reviews describing siRNA delivery systems in detail have recently been published.[7−14]

In this report, we introduce a nanomedicine capable of encapsulating siRNA and then delivering it through the bloodstream to tumor models in mice. This micellar siRNA delivery system was prepared using a block copolymer containing features to improve micelle stability and biological activity. Block copolymer chemistry was chosen based on our previous work with poly(ethylene glycol)-*block*-poly(L-lysine) (PEG-*b*-PLL) containing lysine amines modified with 2-iminothiolane (2IT). We found that this polymer formed nanosized micelle structures with siRNA, which prolonged blood circulation; however, RNAi activity was low.[15,16] Here, we further improved the performance of micelles by incorporating a short peptide on the micelle surface to enhance cell uptake and distribution of siRNA on the subcellular and whole organism levels. Specifically, we used the cyclo-arginine-glycine-glutamic acid (cRGD) peptide, which binds to integrin receptors that are displayed on the surface of several types of tumors and also endothelial cells associated with growing tumors.[17−20] Addition of the cRGD peptide to the micelle structure resulted in a targeted nanoparticle capable of directing siRNA to the site of activity, improving tumor accumulation and cell uptake following intravenous injection. We found that the cRGD-containing micelles improved siRNA activity both *in vitro* and *in vivo* through a combination of improved cell uptake, broadened subcellular distribution, blood stability, and tumor accumulation.

RESULTS AND DISCUSSION

Design and Synthesis of Block Copolymers. Formation of micelles with siRNA requires a material capable of binding a large polyanion and also directing assembly into higher ordered multimolecular structures. Such necessities can be fulfilled by block copolymers, which contain regions of distinctly different chemistries tailored to meet functional demands. Block copolymers used to facilitate micelle formation with siRNA in this work were designed and synthesized to contain three basic features: (i) a cationic segment with thiol groups, (ii) a hydrophilic and biologically benign segment, and (iii) a cell-surface-targeting moiety. This polymer design facilitates micelle formation following electrostatic interaction between oppositely charged macromolecules, resulting in charge neutralization and self-assembly into micelle structures with siRNA contained in the core which is surrounded by a PEG shell. Since polymers and siRNA self-assemble into core−shell micelle structures, modification of the distal end of PEG allows presentation of bioactive moieties, such as the cRGD peptide, on the micelle surface. Chemically, these features were produced from an acetal-PEG-*b*-PLL block copolymer, with the PLL segment serving as the siRNA binding region and also the point of chemical modification by reaction with lysine amines. Acetal functionality contained on the PEG terminus provided a protected aldehyde that was regenerated at low pH to provide the site of attachment for the cRGD peptide by reaction with an N-terminal cysteine residue.[21]

In our previous work, we found that PEG-*b*-PLL alone does not form stable micelle structures with siRNA, so we further modified PEG-*b*-PLL amines with 2IT to introduce amidines and free thiols into the lysine segment of the block copolymer. This modification was aimed to improve the stability of micelle structures through disulfide cross-linking in the core, which can also provide environment-sensitive stabilization of micelle structures following reduction of the covalent disulfide cross-links by free thiols in solution. Disulfide reduction is likely to occur faster within cells than in the bloodstream due to higher glutathione concentrations inside of cells, thus offering site-specific siRNA release functionality.[22] While 2IT modification of PEG-*b*-PLL resulted in the introduction of thiol groups, it also resulted in the formation of cyclic N-substituted 2-iminothiolane ring structures in the lysine side chains, which also showed a micelle-stabilizing effect.[16]

The overall synthesis scheme for preparation of modified polymers starting from acetal-PEG-*b*-PLL (PEG M_w = 12 000, PLL degree of polymerization = 45) is shown in Scheme 1. First, acetal-PEG-*b*-PLL was reacted with excess cRGD peptide at pH 4.0 to produce the peptide−polymer conjugate *via* thiazolidine ring formation between the aldehyde generated on PEG and the N-terminal cysteine residue contained on the cRGD peptide. Analysis of the peptide−polymer conjugate by ^{1}H NMR showed that the reaction was successful, with the appearance of cRGD benzyl protons (D-phenyl alanine) observed (Figure 1A). Further analysis of the integration values determined that ~80% of polymer chains contained conjugated cRGD.

Next, cRGD-PEG-*b*-PLL or acetal-PEG-*b*-PLL was reacted with 2IT to produce cRGD-PEG-*b*-PLL(2IT) and PEG-*b*-PLL(2IT), respectively. For simplicity, polymers

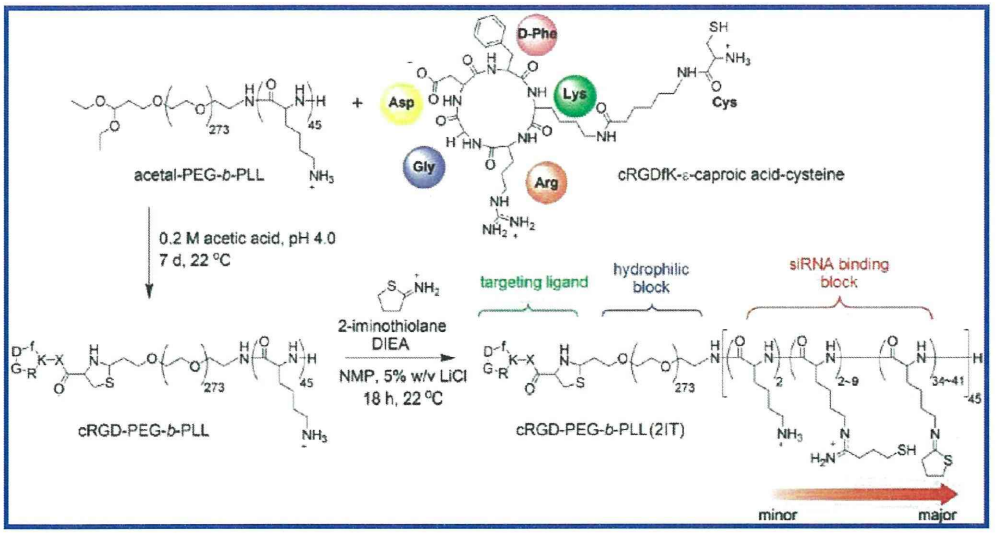

Scheme 1. Modification of PEG-*b*-PLL with cRGD and 2-iminothiolane.

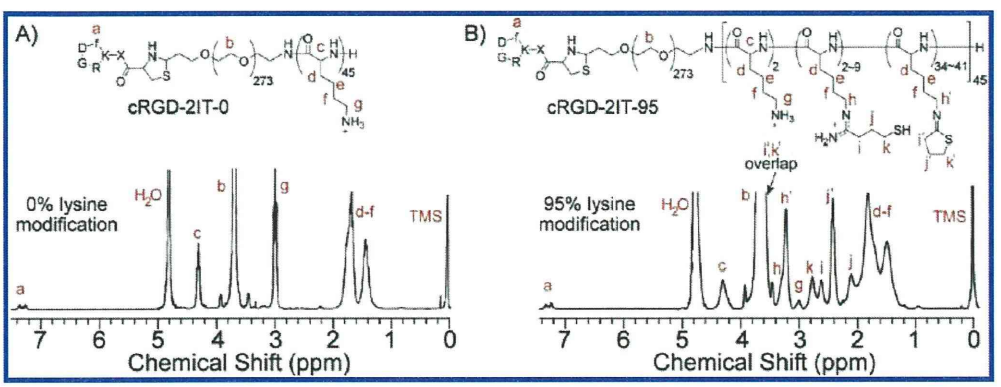

Figure 1. Characterization of polymer products. (A) ^{1}H NMR spectrum of cRGD-PEG-*b*-PLL recorded in D_2O. (B) ^{1}H NMR spectrum of cRGD-PEG-*b*-PLL(2IT) recorded in D_2O containing 3 μL/mL 35% DCl. Polymer composition was estimated based on the ^{1}H NMR spectrum and also results of Ellman's assay shown in Table 1.

are denoted as *X*2IT-*Y*, with "*X*" indicating the presence of the cRGD peptide and "*Y*" indicating the degree of 2IT modification. Polymer modification proceeded *via* nucleophilic reaction of lysine amines with 2IT in the presence of an organic base, with ~2.4 molar equiv of 2IT needed for nearly complete conversion of lysine amines. The degree of 2IT modification was determined to be 95% by ^{1}H NMR analysis, using the ratio of integration values of lysine β, γ, and δ-methylene protons ($(CH_2)_3$, δ = 1.3–1.9 ppm) to values corresponding to 2IT moieties (Figure 1B). Reaction of lysine amines with 2IT generated both 1-(4-mercaptobutyl)-amidine and cyclic iminothiolane functional groups in the PLL segment of the block copolymer, and cyclic iminothiolanes were the major product (~80%) under the reaction conditions used here. Ellman's assay for free thiols revealed a polymer thiol content much lower than the degree of lysine modification, which is consistent with iminothiolane ring formation as this functional group lacks free thiols.

TABLE 1. Summary of Polymer Compositions

polymer	MW[a]	2IT modified lysines (%)[a]	free thiol content (% side chains)[b]
2IT-0	19500	0	0.08 ± 0.04
cRGD-2IT-0	20300	0	0.5 ± 0.07
2IT-95	21800	95	4.6 ± 1.6
cRGD-2IT-95	22500	95	5.1 ± 0.7

[a] Calculated from ^{1}H NMR integration values. [b] Determined by Ellman's assay.

Preparation of Micelles. Micelle structures formed spontaneously upon mixing block copolymer with siRNA, and the theoretical configuration of the particle showing siRNA in the core, a PEG shell, and the cRGD peptide on the micelle surface is depicted in Figure 2A. Micelle formulations are named based on the polymer used for preparation (Table 2.) Micelle formation behavior was different between 2IT modified and unmodified polymers, as scattered light intensity (SLI) analysis showed that micelle structures only formed

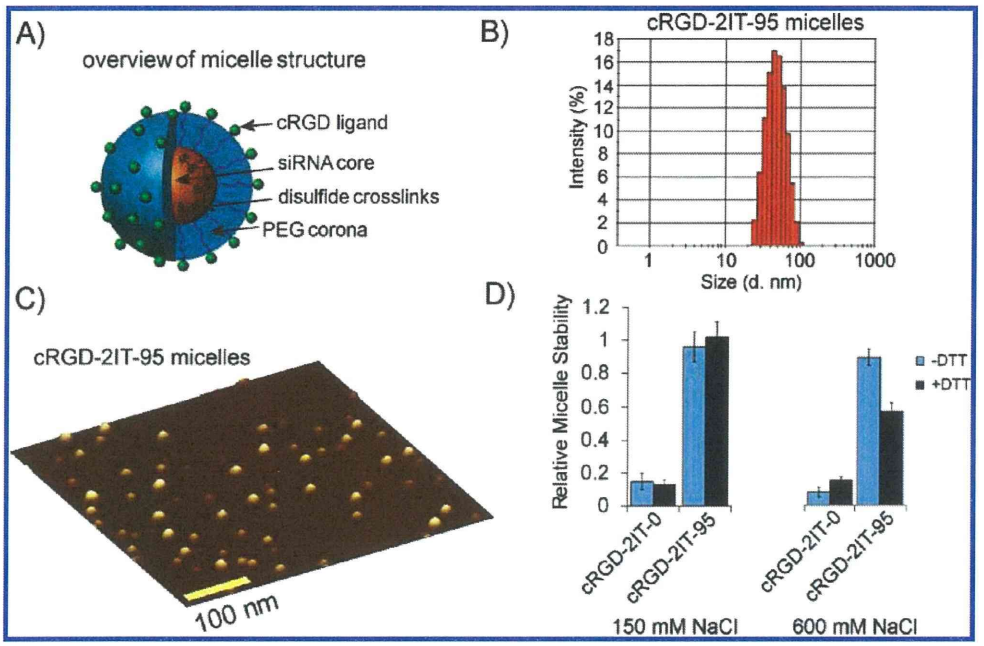

Figure 2. Micelle structure and properties. (A) Schematic representation of polymeric micelle structure and key components. (B) Size distribution histogram of cRGD-2IT-95 micelles determined by dynamic light scattering showing narrowly dispersed particles. (C) Atomic force microscopy image of cRGD-2IT-95 micelles showing spherical structures. (D) Enhancement of micelle stability by 2IT modification of PEG-*b*-PLL at 150 mM and 600 mM NaCl with or without dithiothreitol (a disulfide reducing agent) as determined by light scattering intensity analysis. Micelles prepared with cRGD-2IT-95 were cross-linked prior to analysis.

TABLE 2. Micelle Properties

polymer	polymer/siRNA (moles)	size (*d*, nm)[b]	PDI[b]	ζ-potential[c]	free thiol content (%)[d]
2IT-0	1.2	194 ± 15	0.45 ± 0.09	ND	ND
cRGD-2IT-0	1.2	160 ± 15	0.44 ± 0.06	ND	ND
2IT-95[a]	7.6	45 ± 2	0.09 ± 0.03	−1.99 ± 0.55	1.7 ± 0.9
cRGD-2IT-95[a]	7.6	45 ± 3	0.09 ± 0.03	−0.55 ± 0.91	2.0 ± 0.7

[a] Micelles cross-linked before analysis. [b] Determined by dynamic light scattering. [c] Determined by laser Doppler electrophoresis. [d] Determined by Ellman's assay.

at the specific molar ratio of polymer/siRNA of 1.2 (also near the charge-neutral point) for unmodified polymers, while 2IT modified polymers formed micelles with siRNA over a broad range of polymer/siRNA molar ratios until a plateau in SLI was observed at the polymer/siRNA molar ratio of ~8 (Table 2 and Supporting Information). Formation of micelle structures with siRNA in the presence of higher molar ratios of polymer compared to the parent PEG-*b*-PLL is a characteristic of the 2IT-95 polymer and is consistent with our previous reports.[15,16] The shift in the polymer/siRNA molar ratio for micelle formation with the 2IT-95 polymer reflects the presence of cyclic N-substituted 2-iminothiolane structures in the siRNA binding segment of the block copolymer. The imine groups contained in the N-substituted 2-iminothiolane ring has a lower pK_a than amidines (~6–7 *vs* ~11–12), which results in reduced polymer charge at pH 7.4.[23] This heterocyclic functional group also contains features that could allow for other non-electrostatic binding modes with siRNA, allowing micelle formation over a broad range of polymer/siRNA ratios. Specifically, N-substituted 2-iminothiolane rings are more hydrophobic than unmodified lysines, contain a dipole moment between C–S and C–N bonds, and also contain an imine nitrogen. These characteristics could lead to enhanced van der Waals and dipole–dipole interactions as well as hydrogen bonding capability with siRNA or with other polymer chains associated within micelle structures. On the other hand, the optimal polymer/siRNA molar ratio for particle formation with PEG-*b*-PLL containing unmodified lysine residues was very sensitive to the amount of polymer, suggesting that excess cationic charge interferes with micelle formation. 2IT-95 (both with and without cRGD) polymer generally produced higher quality micelles with smaller size and narrow size dispersion, demonstrating improved control of micelle assembly (Figure 2B).

On the basis of these light scattering results, the optimal micelle formation conditions were defined as the molar ratio of polymer/siRNA that resulted in the

maximum SLI, indicating formation of multimolecular micelle structures. Micelles were prepared at the polymer/siRNA molar ratios shown in Table 2 and, in the case of 2IT modified polymers, cross-linked before use. Micelle cross-linking was achieved by dialysis in HEPES buffer containing DMSO, which is a mild oxidant of free thiols.[24] Reduced polymer thiol content following the oxidation procedure confirmed that disulfide formation occurred (Table 2). Direct observation of cross-linked micelles by atomic force microscopy (AFM) revealed spherical structures approximately 15–20 nm in size, which is smaller than the hydrodynamic diameter determined by light scattering measurement and probably more indicative of the micelle core size (Figure 2C). Calculation of the theoretical micelle diameter assuming that the AFM image represents the micelle core results in a value similar to DLS results, as the height of a 12K PEG in the mushroom configuration is ~9 nm, thus, ~20 nm + (~9 nm × 2) = ~38 nm.[25] Furthermore, the micelle diameters determined by light scattering measurement were expressed as *z*-averaged diameters. Conversion of DLS data to the number-averaged diameter yields ~32 nm, which is in good agreement with the theoretical diameter calculated from the AFM image. Analysis of particle ζ-potentials demonstrated that micelle structures were nearly neutral in charge, which is consistent with the formation of core–shell micelle structures (Table 2).

Modification of PEG-*b*-PLL with 2IT increased the stability of micelles prepared with siRNA, as evidenced by SLI measurement of micelle solutions at different ionic strengths (Figure 2D). Increased ionic strength is expected to shield the charge of siRNA and disrupt electrostatic interactions, leading to dissociation of unstable micelle structures and decreased SLI. cRGD-2IT-0 micelles nearly completely dissociated at 150 mM NaCl (physiological ionic strength), whereas cRGD-2IT-95 micelles remained largely intact at both 150 and 600 mM NaCl. Addition of the disulfide reducing agent dithiothreitol (DTT) to solutions of cRGD-2IT-95 micelles resulted in a decrease in SLI at 600 mM NaCl, showing that disulfide cross-linking contributed to micelle stability. However, ~60% of the SLI intensity was retained for cRGD-2IT-95 micelles in the presence of DTT at 600 mM NaCl, suggesting that the iminothiolane ring structure is also important for micelle stability. It should be noted that a polymer similar to cRGD-2IT-95 containing only amidines and thiols in the polymer structure, and lacking N-substituted 2-iminothiolane rings, nearly completely dissociated under the same conditions in the presence of DTT.[16] Additionally, the presence of the cRGD peptide did not affect micelle stability in this assay (Supporting Information). For all experiments described hereafter, micelle formulations were prepared for each polymer at the optimal polymer/siRNA molar ratio indicated in Table 2 and, in the case of 2IT-95 and cRGD-2IT-95 formulations, cross-linked before use.

***In Vitro* Gene Silencing.** Polymeric micelles were analyzed for their ability to inhibit protein expression in cultured HeLa cells using a luciferase assay. HeLa cells express $\alpha_v\beta_3$ and $\alpha_v\beta_5$ integrin receptors that can bind the cRGD peptide, and thus are appropriate for use in this study to determine the effects of the cRGD peptide on micelle performance.[26,27] Micelle encapsulation of siRNA within stable structures containing cRGD is expected to increase the internalization of siRNA into cells and improve gene silencing efficacy. Micelles prepared with siRNA-targeting luciferase mRNA for degradation were administered to HeLa cells stably expressing GL3 luciferase (HeLa-luc), and cell luminescence was measured over time. Polymeric micelle formulations lacking the cRGD peptide were ineffective at decreasing cell luminescence; however, micelles prepared from polymer modified with both 2IT and cRGD showed a marked decrease in cell luminescence after 50 h incubation (Figure 3A). Further analysis of cells treated with cRGD-2IT-95 micelles showed that luminescence intensity gradual decreased over the entire 50 h of the experiment, suggesting that siRNA was slowly released into the site of activity in the cell cytoplasm (Figure 3B). No reduction in luminescence occurred when off-target siRNA was contained in cRGD-2IT-95 micelles, suggesting that reduced luminescence observed for cells treated with target siRNA was due to sequence-specific gene silencing (Figure 3A,B). cRGD-2IT-95 micelles were less effective than the commercial transfection reagent RNAiMax employed as the positive control. However, this lipid-based siRNA delivery agent achieves high efficacy *in vitro* by directly transporting siRNA across the exterior cell membrane, thus avoiding cell uptake and trafficking barriers encountered with PEGylated micelles.[28]

The chemical structure of the siRNA binding segment in the block copolymer used to prepare micelles was critical to realize performance gain due to the cRGD peptide, as only the cRGD-2IT-95 formulation showed activity. This demonstrates the importance of stable micelle structures, which may allow for multiple cRGD peptides to be presented in a single particle and improve binding to cell-surface integrin receptors. The importance of cRGD density was further investigated by preparing cRGD-2IT-95 micelles with reduced cRGD content. cRGD-2IT-95 micelles prepared at the polymer/siRNA molar ratio of 4 or by mixing cRGD-2IT-95 and 2IT-95 polymers before micelle formation with siRNA (polymer/siRNA molar ratio = 7.6) were less effective at reducing gene silencing (Figure 3C), which suggests that high cRGD content was necessary for effective micelle formulations.

Analysis of micelle toxicity following incubation in HeLa-luc cells showed that micelles were well tolerated, as cell metabolism was maintained at high levels

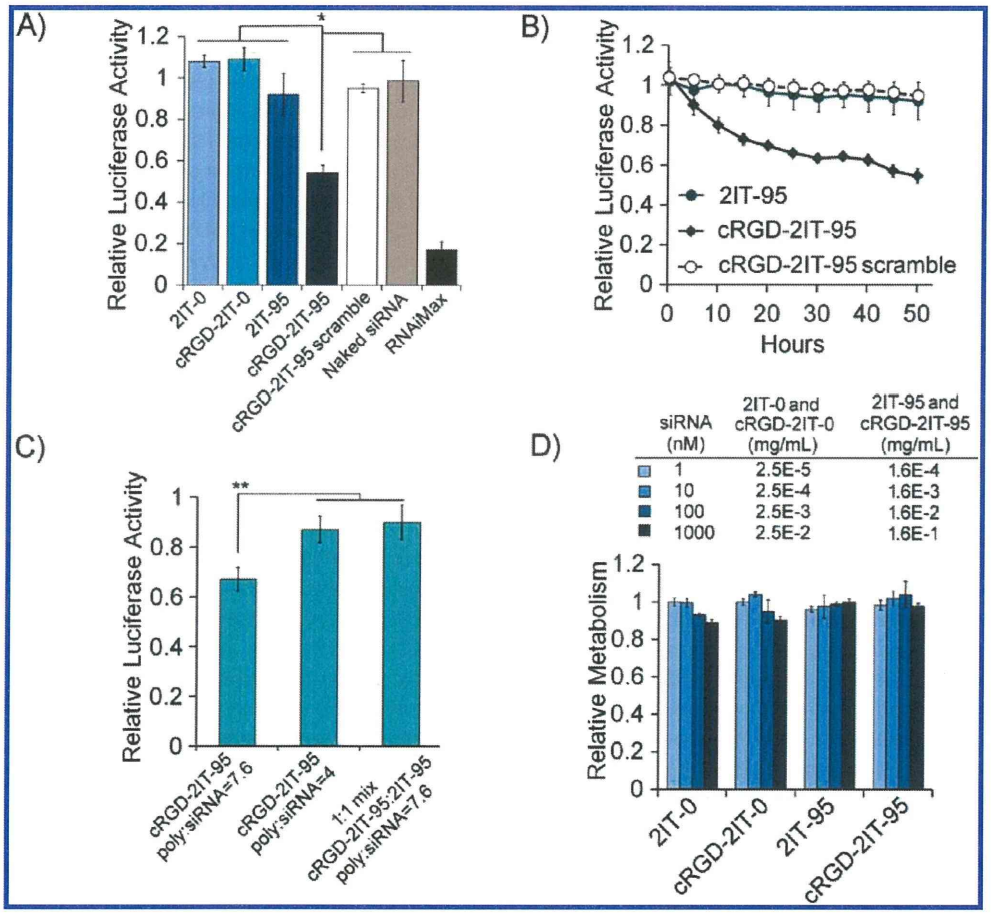

Figure 3. Gene silencing ability of siRNA micelles and tolerance in HeLa-luc cancer cells. (A) Quantification of luciferase luminescence following incubation with micelles containing antiluciferase siRNA (or scramble siRNA as noted in legend). Micelles were prepared at the optimal polymer/siRNA ratio shown in Table 2 and administered at a siRNA concentration of 200 nM, while RNAiMax was administered at a concentration of 10 nM. All samples were incubated for 50 h, $n = 4$, $*p < 0.001$. (B) Time dependence of luminescence reduction for cRGD-2IT-95 micelles, 200 nM siRNA, $n = 4$. (C) Activity of cRGD-2IT-95 micelles prepared at non-optimal conditions. Micelles were prepared at the polymer/siRNA molar ratio of 4 or mixed 1:1 with 2IT-95 polymer before micelle formation with siRNA (polymer/siRNA molar ratio = 7.6) and subsequent cross-linking. All samples were incubated for 50 h, 200 nM siRNA, $n = 4$, $**p < 0.005$. (D) Toxicity of micelles toward HeLa-luc cells (48 h) at different concentrations. The concentrations of siRNA and polymer are denoted in the legend.

for all polymeric micelle formulations even at concentrations 5 times higher than that used for gene silencing experiments (Figure 2D). These results further support that reduced luminescence observed for the cRGD-2IT-95 micelle formulation was due to the specific inhibition of luciferase expression and not an artifact of reduced cell luminescence due to cytotoxicity.

Cell Uptake and Trafficking of Micelles. Initial screening of polymeric micelle formulations *in vitro* revealed that high micelle stability and high cRGD content were linked to improved gene silencing activity. One possible reason for the improved activity observed for cRGD-2IT-95 micelles is higher cell uptake due to the improved interactions with the cell surface. PEGylation of nanoparticles in general creates a unique dilemma, as both benefits and detriments result. PEG reduces nonspecific interactions between particles with each other and components in biological milieu, preventing aggregation or nonspecific binding to off-target species. However, this also reduces interactions with cell surfaces, leading to lower uptake. In this study, installation of the integrin-targeting cRGD peptide was aimed to increase cell uptake due to improved cell-surface interactions.

Cellular uptake of micelles was determined by flow cytometric analysis of HeLa-luc cells following incubation with micelles prepared with fluorescent-labeled siRNA (Figure 4). No improvement in cell uptake due to the cRGD peptide was observed for cRGD-2IT-0 micelles, while the cRGD-2IT-95 micelle formulation showed a shift in the cell population toward higher fluorescence intensity compared to 2IT-95 micelles, demonstrating increased uptake of siRNA. This corroborates well with *in vitro* gene silencing results, where 2IT-0 formulations showed no difference in gene silencing between (+) and (−) cRGD formulations.